

Origin of rotational kinematics in the globular cluster system of M31: A new clue to the bulge formation

Kenji Bekki^{1*}

¹*School of Physics, University of New South Wales, Sydney, NSW, 2052, Australia*

Accepted, Received 2005 February 20; in original form

ABSTRACT

We propose that the rotational kinematics of the globular cluster system (GCS) in M31 can result from a past major merger event that could have formed its bulge component. We numerically investigate kinematical properties of globular clusters (GCs) in remnants of galaxy mergers between two disks with GCs in both their disk and halo components. We find that the GCS formed during major merging can show strongly rotational kinematics with the maximum rotational velocities of $\sim 140 - 170$ km s⁻¹ for a certain range of orbital parameters of merging. We also find that a rotating stellar bar, which can be morphologically identified as a boxy bulge if seen edge-on, can be formed in models for which the GCSs show strongly rotational kinematics. We thus suggest that the observed rotational kinematics of GCs with different metallicities in M31 can be closely associated with the ancient major merger event. We discuss whether the formation of the rotating bulge/bar in M31 can be due to the ancient merger.

Key words: Magellanic Clouds – galaxies:structure – galaxies:kinematics and dynamics – galaxies:halos – galaxies:star clusters

1 INTRODUCTION

The structural and kinematical properties of GCSs are considered to provide valuable information on the formation and evolution of their host galaxies (e.g., Searle & Zinn 1978; Romanowsky et al. 2009). Recent observational studies on kinematical properties of GCSs in galaxies and their comparison with theoretical and numerical works have advanced our understanding on mass distributions of galaxies (e.g., Pierce et al. 2006; Romanowsky et al. 2009), formation of elliptical galaxies (e.g., Bekki et al. 2005), and formation and evolution of dwarf galaxies (e.g., Beasley et al. 2009). A growing number of observational data sets on kinematical properties of GCSs have been now accumulated not only for galaxies in the local group but also for nearby galaxies (Brodie & Strader 2006 for a recent review) so that we can discuss formation processes of their host galaxies and their dependences on galactic global properties (e.g., Hubble types) in more detail based on the observations.

One of the intriguing properties of GCSs in galaxies is the observed rotational kinematics of the GCS in M31 (e.g., Huchra et al. 1982; Perrett et al. 2002). Recent wide-field surveys of the GCS in M31 (Lee et al. 2008)

have confirmed that the GCS composed both of metal-poor ($[\text{Fe}/\text{H}] < -0.9$ in their criterion) and metal-rich ($[\text{Fe}/\text{H}] > -0.9$) objects has a rotational amplitude of ~ 190 km s⁻¹. Such kinematics are in a striking contrast with the low rotation of the Galaxy's GCS (e.g., Armandroff 1989) with an origin that remains unclear.

The purpose of this paper is to discuss (i) why the GCS of M31 shows such a large amount of rotation and (ii) what implications it has for the formation and evolution of M31. Previous numerical works showed that rotational kinematics of GCSs in elliptical galaxies can be due to past major merger events that formed the galaxies (e.g., Hernquist & Bolte 1993; Bekki et al. 2005). We thus consider that the rotational kinematics of the GCS is closely associated with a major merger event in M31 long ago and thereby investigate whether galaxy merging can reproduce well the observed kinematics of the GCS. We also discuss whether the observed rotating bulge/bar in the M31 (e.g., Beaton et al. 2007) can be due to the major merger event responsible for the formation of the GCS with rotational kinematics.

* E-mail: bekki@phys.unsw.edu.au

Table 1. The values of model parameters and a brief summary of the results

model	$M_{\text{dm}}/M_{\text{d}}$ ^a	m_2 ^b	r_{p} ($\times R_{\text{d}}$) ^c	e_{p} ^d	orbital ^e	$V_{\text{max,dgc}}$ (km s ⁻¹) ^f	$V_{\text{max,hgc}}$ (km s ⁻¹) ^g	comments
1	9	1.0	2.0	0.72	PP	136	123	the standard model
2	9	1.0	2.0	0.72	PR	114	133	
3	9	1.0	1.0	0.85	PP	95	92	
4	9	0.5	2.0	0.72	PP	107	38	unequal-mass merger
5	19	1.0	2.0	0.72	PP	174	91	

^a The mass ratio of dark matter halo to stellar disk in a galaxy.

^b The mass ratio of two disks in a galaxy merger.

^c The pericenter distance of a merger in units of the disk size R_{d} .

^d The orbital eccentricity of a merger.

^e “PP” and “PR” represent prograde-prograde and prograde-retrograde merging, respectively.

^f The maximum rotational velocity of DGCs (GCs initially in disks) in a merger remnant.

^g The maximum rotational velocity of HGCs (GCs initially in halos) in a merger remnant.

2 THE MODEL

Since the numerical methods and techniques we employ for modeling dynamical evolution of mergers between two disks with GCs have already been detailed elsewhere (Bekki et al. 2005; Bekki & Forbes 2006), we give only a brief review here. The progenitor disk galaxies that take part in a merger are given a dark halo, a thin exponential disk, and GCs initially in disks (referred to as “DGCs” from now on) and in halos (“HGCs”). The total mass and size of an exponential disk with no bulge are M_{d} and R_{d} , respectively.

We consider that the total stellar mass of a merger remnant should be similar to the total mass (M_{b}) of the present bulge of M31 ($M_{\text{b}} = 3 - 4 \times 10^{10} M_{\odot}$; e.g., Seigar et al. 2008; Geehan et al. 2006). We thus adopt $M_{\text{d}} = 2 \times 10^{10} M_{\odot}$ as a reasonable value in the present study. We adopt the density distribution of the NFW halo (Navarro, Frenk & White 1996) with the mass of M_{dm} and a concentration parameter determined by M_{dm} according to the formula derived by recent CDM simulations (e.g., Neto et al 2007). The stellar disk has the scale length (R_0) of $0.2R_{\text{d}}$.

The present bulge-less disk model would be reasonable for less massive disk galaxies with no/little bulges like the Large Magellanic Cloud and Magellanic-type galaxies with total masses of $\sim 10^{10} M_{\odot}$, but it would not be so realistic for luminous disk galaxies like the merger progenitor disks of M31. We however conjecture since the bulge masses are quite small in comparison with total masses of galaxies (inclusive of dark matter halos), final kinematics of GCSs in merger remnants would not depend strongly on whether or not we include bulges in initial disks. Thus, as long as we mainly discuss global kinematical properties of GCSs in merger remnants, the present model can be regarded as an appropriate one.

Previous observations revealed that less luminous disk galaxies, which are considered to form the bulge component of M31 with rotational kinematics of the GCS in the present study, have disky distributions with rotational kinematics in their GCs (e.g., Freeman et al. 1983; Olsen et al. 2004). We thus consider the presence of DGCs in merger progenitor disks in the present study: DGCs were not considered in our previous works (e.g., Bekki et al. 2003a; 2005) and such DGCs with strongly rotational kinematics are not observed in the metal-rich GCs of the Galaxy. The DGCs have the same exponential distribution and rotational kinematics as

field stars in the stellar disk of their host galaxy. The initial rotational amplitude of DGCs is $\sim 170 \text{ km s}^{-1}$ for $M_{\text{d}} = 2 \times 10^{10} M_{\odot}$ and $M_{\text{dm}}/M_{\text{d}} = 9$.

The Galactic HGCs and the stellar halo have similar radial density profiles of $\rho(r) \propto r^{-3.5}$ (van den Bergh 2000). We therefore assume that the HGCs in our galaxies have a power-law profile with an exponent of -3.5 and a half-number radius of $1.4R_0$ (which is $\sim 5 \text{ kpc}$ for the Galaxy and thus consistent with observations). The HGCs are assumed to have isotropic velocity dispersions determined by the mass distribution of the galaxy. Total numbers of DGCs and HGCs in a galaxy are set to be 100 and 100, respectively.

The mass ratio of the two disks (m_2) in a merger is assumed to be a free parameter. In all of the simulations of pair mergers, the orbit of the two disks is set to be initially in the xy plane and the distance between the center of mass of the two disks is assumed to be $12R_{\text{d}}$. The pericenter distance (r_{p}) and the eccentricity (e_{p}) in a pair merger are assumed to be free parameters that control orbital energy and angular momentum of the merger. The spin of each galaxy in a merger is specified by two angles θ_i and ϕ_i , where suffix i is used to identify each galaxy. θ_i is the angle between the z axis and the vector of the angular momentum of a disk. ϕ_i is the azimuthal angle measured from the x axis to the projection of the angular momentum vector of a disk onto the xy plane.

We mainly show the results of “the standard model” with $M_{\text{d}} = 2 \times 10^{10} M_{\odot}$, $M_{\text{dm}}/M_{\text{d}} = 9$, $m_2 = 1$, $r_{\text{p}} = 2R_{\text{d}}$, $e_{\text{p}} = 0.72$, $\theta_1 = 30^\circ$, $\theta_2 = 45^\circ$, $\phi_1 = 45^\circ$, and $\phi_2 = 120^\circ$. We describe the results of this standard model with an orbital configuration similar to “prograde-prograde” merging (in which the orbital spin axis of the merger is parallel to intrinsic spin axes of the two disks), mainly because the final GCS can clearly show strongly rotational kinematics as observed in M31. We also show the results of the model with a “prograde-retrograde” orbital configuration in which $\theta_2 = 225^\circ$ and other parameters are exactly the same as those in the standard model.

In order to discuss the origin of the central bar/bulge of M31, we investigate in which models the merger remnants show rotating stellar bars. Although we investigate 34 models, we show the results of five representative models which either show clearly rotating bars or have no such rotating components in merger remnants: comparison between these models enables us to understand better the role of an an-

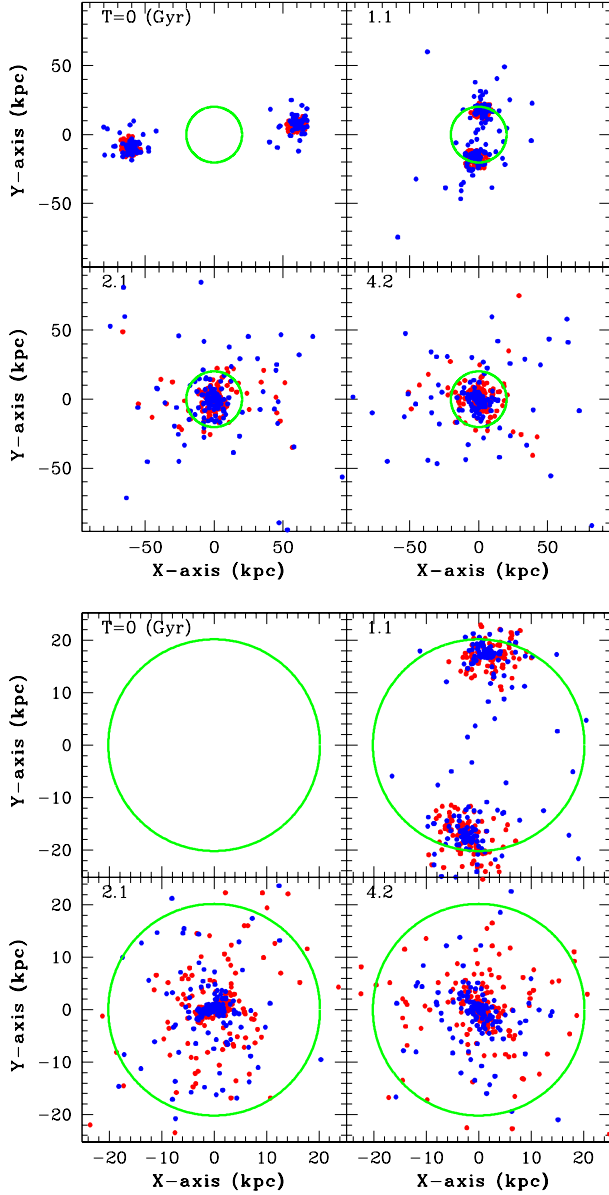


Figure 1. Distributions of disk GCs (DGC, red) and halo ones (HGC, blue) of a galaxy merger projected onto the x - y plane (i.e., orbital plane of the merger) for larger (upper) and smaller (lower) scales of view in the standard model. The time T shown in the upper left corner of each panel indicates the time that elapsed since the simulation starts. Green circles indicate 20 kpc from the mass center of the merger.

cient merger event in the formation of the bulge component in M31.

The model parameters and some brief results are given in the Table 1. The total particle number for a major merger in a simulation is 10^6 and the simulation is carried out on the latest version of GRAPE (GRAVity PipE, GRAPE-7) which is the special-purpose computer for gravitational dynamics (Sugimoto et al. 1990). In estimating the GCS kinematics, the merger remnant is viewed near to edge-on, and binned major-axis profiles are constructed. In order to have enough objects in each bin, GCs at all minor axis distances are included, which also approximately replicates the comparison

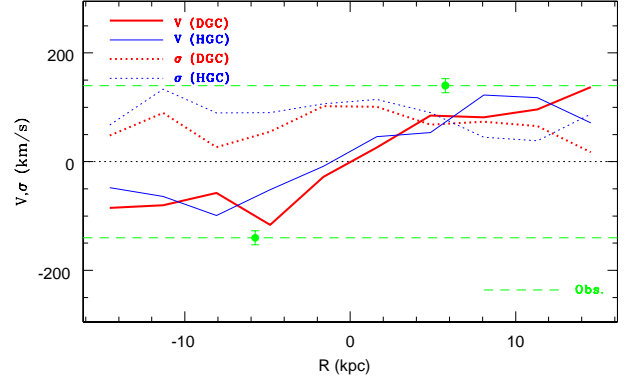


Figure 2. Radial profiles of line-of-sight velocities (V , solid) and velocity dispersions (σ , dotted) for DGCs (red) and HGCs (blue) for the merger remnant at $T = 4.2$ Gyr in the standard model. The dotted horizontal black line represents $V(\sigma) = 0 \text{ km s}^{-1}$. The observed $v_{\text{rot}} \sim 140 \text{ km s}^{-1}$ for the full sample of GCs in M31 (Perrett et al. 2002) is shown by a dashed green line for comparison: Lee et al (2008) show significantly larger v_{rot} ($\sim 188 \text{ km s}^{-1}$) of the GCS for $|Y| \geq 0 \text{ kpc}$. The locations of the filled circles indicate where the observed velocity profile becomes flat and the error bars are observational ones ($\pm 13 \text{ km s}^{-1}$).

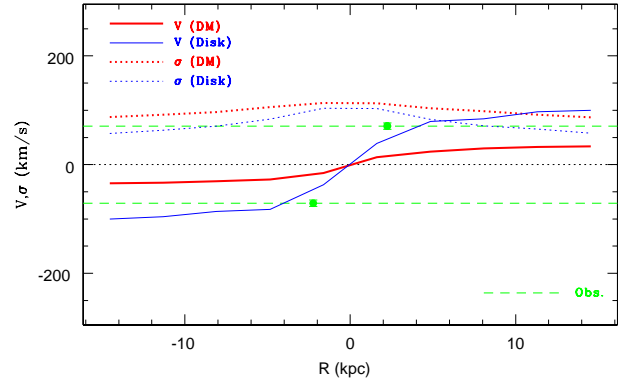


Figure 3. The same as Fig. 2 but for dark matter (red) and disk stars (blue). The bulge observational results are from McElroy (1983) and the locations of the filled circles indicate the observed outermost region ($R = 9.76'$) at the position angle of 45° .

observations. Formation of metal-rich GCs through dissipative gas dynamics of galaxy merging (e.g., Bekki et al. 2002) and adiabatic contraction of the GCS in M31 due to later massive growth of the disk component could increase appreciably the rotational amplitude V of the GCS. The quantitative estimation of this effect is not done here and will be done in our future studies. It should be stressed that this paper is meant to be schematic rather than reproducing the observed galaxy in a fully self-consistent manner.

3 RESULTS

Fig. 1 shows that both DGCs and HGCs can be spatially mixed to form a new GCS during violent dynamical relation that results in transformation from two disks into one spheroidal galaxy. Owing to angular momentum redistribution during major merging, not only HGCs but also DGCs

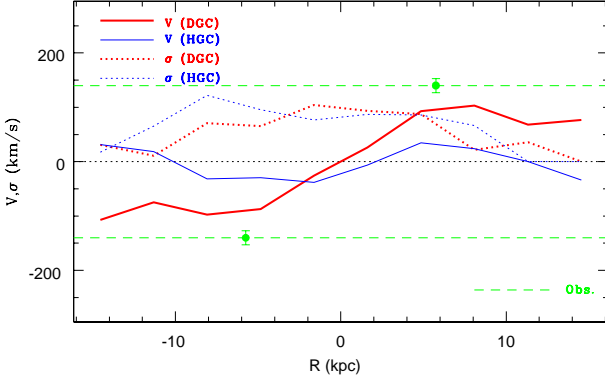


Figure 4. The same as Fig. 2 but for the model with $m_2 = 0.5$.

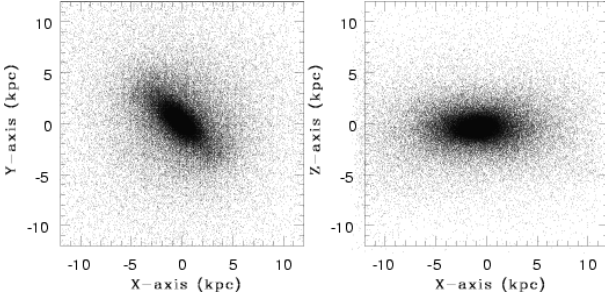


Figure 5. Distributions of stars projected onto the x - y (left) and x - z (right) planes at $T = 4.2$ Gyr in the standard model. Only one for every ten particles is shown for clarity.

can be transferred to the outer halo region and thus seen there in the merger remnant. The half-number radii for the DGCs and the HGCs are both ~ 5.0 kpc in the merger remnant, which is consistent with the observations by Battistini et al. (1993). As the stellar remnant shows a rotating bar (discussed later in §4), DGCs and HGCs also show barred structures, appreciably flattened shapes (qualitatively consistent with observations), and figure rotation.

Fig. 2 clearly shows global rotation both in DGCs and HGCs, though the radial profiles of V and σ do not smoothly change owing to the small numbers of GCs at each bin. The maximum V (V_{\max}) and σ (σ_{\max}) for DGCs (HGCs) within the central 16 kpc are 136 km s^{-1} (123 km s^{-1}) and 102 km s^{-1} (106 km s^{-1}), respectively. Therefore V_{\max}/σ_{\max} for DGCs and HGCs are 1.3 and 1.2, respectively, which means that the final GCS has strongly rotational kinematics. The velocity profile becomes flat ($V \sim 100 \text{ km s}^{-1}$) at $R \sim 4$ kpc. The simulated two-dimensional line-of-sight velocity map of the GCS shows clearly global rotation.

We here compare the simulated rotational kinematics with the observed one in M31 (e.g., $V = 138 \pm 13 \text{ km s}^{-1}$ in Perrett et al. 2002). Observational error bars in V are not so small and V ranges from 98 km s^{-1} to 188 km s^{-1} for $0 \text{ kpc} \leq |Y| \leq 5 \text{ kpc}$ (Lee et al. 2008), where $|Y|$ is the projected vertical distance from the M31 disk plane. The simulated rotational amplitude of the GCS is slightly smaller than the observed one by Perrett et al. (2002): It should be noted that the observational results depend on the details of how the data are binned and fitted.

We consider that the best model needs to reproduce the above V of $\sim 140 \text{ km s}^{-1}$. Fig. 3 shows that even the dark

matter halo of the merger remnant can have a small amount of rotation ($V \sim 34 \text{ km s}^{-1}$) owing to the redistribution of angular momentum (i.e., conversion of orbital angular momentum of merging two galaxies into internal one of the merger remnant). This result suggests that if the two galaxies have hot gaseous halos, then the remnant is highly likely to have a slowly rotating gaseous halo. Fig. 3 also shows that the stellar component of the merger remnant has a significant amount of rotation ($V_{\max} \sim 100 \text{ km s}^{-1}$), which means that the spheroid is rapidly rotating (i.e., rotating bulge is formed from major merging).

The reason for the smaller V of the dark matter halo in comparison with the GCS is due largely to the difference in the initial spatial distribution between the halo and the GCS, demonstrating that GC rotation would not be used to infer dark matter halo rotation. The inner part of the merger can more strongly spin-up during and after major merging owing to (i) the prograde-prograde orbital configuration of the merging and (ii) the development of the rotating bar. The distribution of the GCS in the merger progenitor disk is by a factor of 4 more compact than that of the halo so that the GCS can more strongly spin-up: most of the individual GCs can obtain a larger amount of intrinsic spin angular momentum with respect to the center of the merger remnant.

Fig. 4 shows that strongly rotational kinematics of GCs can be seen only in DGCs in the model with $m_2 = 0.5$ (Model 4): V_{\max} is 107 km s^{-1} for DGCs and 38 km s^{-1} for HGCs. The higher and lower V_{\max} in DGCs and HGCs, respectively, are confirmed in other unequal-mass merger models (e.g., $m_2 = 0.3$). It should be noted here that the model 1 shows only slightly higher V_{\max} in DGCs, which is due to different kinematics between DGCs and HGCs (i.e., *initial* global rotation only in DGCs). These results therefore mean that if metal-poor and metal-rich GCs originate from HGCs and DGCs, respectively, then kinematical properties of GCs in the remnants of galaxy merging with smaller m_2 (or unequal-mass merging) can be significantly different between metal-poor and metal-rich ones. These results furthermore imply that the observed rotational kinematics both for metal-poor and metal-rich GCs in M31 can give some constraints on the mass-ratio (m_2) of two disks in galaxy merging that could have occurred in M31.

The model 1 does not explain well the observed total halo mass: later numerous accretion events of dwarfs with few GCs and stars are required to increase significantly the total mass after the merging. The models with larger $M_{\text{dm}}/M_{\text{d}}$ can show higher V_{\max} in DGCs owing to the initially higher circular velocities of the stellar disks. For example, the model with $M_{\text{dm}}/M_{\text{d}} = 19$ (Model 5) shows $V_{\max} = 174 \text{ km s}^{-1}$ and $\sigma_{\max} = 134 \text{ km s}^{-1}$: it should be stressed here that the total mass of the remnant is $8 \times 10^{11} M_{\odot}$ thus can be more consistent with observations than Model 1 in terms of the total mass of M31. A possible reason for the lower V_{\max} (91 km s^{-1}) for HGCs in the model 5 is that more strongly self-gravitating stellar disks can also play a role in increasing global rotation of HGCs: Such a role is weaker in the model 5 in which the disk is much more weakly self-gravitating.

Models with different orbital configurations can show stronger rotational kinematics in DGCs and HGCs, if larger r_{p} are adopted. For example, the model with a prograde-

retrograde orbital configuration (Model 2) shows $V_{\max} = 114 \text{ km s}^{-1}$ and $\sigma_{\max} = 102 \text{ km s}^{-1}$ but does not show a bar. The models with smaller r_p (e.g., Model 3) show smaller V_{\max} in DGCs, which implies that the observed V_{\max} can give some constraints on the orbital parameters for galaxy merging that occurred in M31. Thus only the models with larger r_p can better reproduce the observed kinematical properties of the M31 GCS.

4 DISCUSSION AND CONCLUSIONS

Fig. 5 shows that the stellar remnant looks like a bar if it is viewed from face-on in the standard model of the present study: the bar is confirmed to have figure rotation. The stellar distribution viewed from edge-on appears to have a flattened spherical body, which can be identified as a bulge. The present study thus implies that M31's observed bulge/bar (e.g., Beaton et al. 2007) can be formed from an ancient major merger event. It should be noted here that dissipative gas dynamics which can determine the final morphological properties of merger remnants (e.g., boxy or disk shapes) is not included in the present study.

If the inner bar/bulge of M31 was really formed from ancient major merging before its disk formation, then the later development of the stellar and gaseous disk may well be significantly influenced by dynamical action of the already formed bar. Also, later slow gas accretion and the resultant disk formation in M31 could change structural and kinematics properties of the already developed GCS to some extent: it would be possible that adiabatic compression of the GCS by later gradual development of the disk can enhance the rotational amplitude of the GCS. It is our future study to numerically investigate disk formation and evolution of M31 under the presence of the already formed bar.

The present work suggests that the hot diffuse halo gas recently detected by *Chandra* (Li & Wang 2007) can have a significant amount of rotation resulting from angular momentum redistribution of the possible major merger. Furthermore, the observed extensive HI cloud population of M31 (e.g., Thilker et al. 2004; Westmeier et al. 2007) can also have rotational kinematics if they originate from stripped HI gas from the merger progenitor disks. Given that major merging can form very extended stellar halos (Bekki et al. 2003b; Bekki & Peng 2006), the observed extended stellar halo in M31 (e.g., Ibata et al. 2007) would have fossil information in the possible ancient major merger event.

If M31 was formed from multiple and sequential merging of dwarf satellites from random directions, it seems to be highly unlikely that the final GCS has a large amount of global rotation. Therefore, if the rotational kinematics of the GCS derived from previous observations is further confirmed by ongoing observational studies, it then suggests that a dramatic physical process is responsible for the observed *globally organized motion* of GCs. Our simulations imply that an ancient major merger of two disks with GCs with different metallicities could be responsible for the enigmatic kinematics of the GCS in M31, as well as the inner bar or bulge.

5 ACKNOWLEDGMENT

I am grateful to the anonymous referee for valuable comments, which contribute to improve the present paper.

REFERENCES

- Armandroff, T. E., 1989, *AJ*, 97, 375
- Battistini, P. L., Bonoli, F., Casavecchia, M., Ciotti, L., Federici, L., Fusi-Pecchi, F., 1993, *A&A*, 272, 77
- Beasley, M. A., Cenarro, A. J., Strader, J., Brodie, J. P., 2009, *AJ*, 137, 5146
- Beaton, R. L., et al. 2007, *ApJ*, 658, 91
- Bekki, K., Forbes, D. A., Beasley, M. A., & Couch, W. J. 2002, *MNRAS*, 344, 1334
- Bekki, K., Forbes, D. A., Beasley, M. A., Couch, W. J. 2003a, *MNRAS*, 344, 1334
- Bekki, K., Harris, W. E., Harris, G. L. H., 2003b, *MNRAS*, 338, 587
- Bekki, K., Beasley, M. A., Brodie, J. P., & Forbes, D. A. 2005, *MNRAS*, 363, 1211
- Bekki, K., Forbes, D. A., 2006, *A&A*, 445, 485
- Bekki, K., Peng, E. W., 2006, *MNRAS*, 370, 1737
- Brodie, J. P., Strader, J., 2006, *ARA&A*, 44, 193
- Freeman, K. C., Illingworth, G., & Oemler, A., Jr., 1983, *ApJ*, 272, 488
- Geehan, J. J., Fardal, M. A., Babul, A., Guhathakurta, P., 2006, *MNRAS*, 366, 996
- Hernquist, L., Bolte, M., 1993, in *The globular clusters-galaxy connection*, ASP, v48, p788 edited by Graeme H. Smith, and Jean P. Brodie,
- Huchra, J., Stauffer, J., van Speybroeck, L., 1982, *ApJ*, 259, L57
- Ibata, R., Martin, N. F., Irwin, M., Chapman, S., Ferguson, A. M. N., Lewis, G. F., McConnachie, A. W., 2007, *ApJ*, 671, 1591
- Lee, M. G., Hwang, H. S., Kim, S. C., Park, H. S., Geisler, D., Sarajedini, A., Harris, W. E., 2008, *ApJ*, 674, 886
- Li, Z., Wang, Q. D., 2007, *ApJ*, 668, L39
- McElroy, D. B., 1983, *ApJ*, 270, 485
- Navarro, J. F., Frenk, C. S., White, S. D. M., 1996, *ApJ*, 462, 563 (NFW)
- Neto, A. F., et al. 2007 *MNRAS*, 381, 1450
- Olsen, K. A. G., Miller, B. W., Suntzeff, N. B.; Schommer, Robert A., Bright, J., 2004, *AJ*, 127, 2674
- Perrett, K. M., et al., 2002, *AJ*, 123, 2490
- Pierce, M. et al. 2006, *MNRAS*, 368, 325
- Romanowsky, A. J., Strader, J., Spitler, L. R., Johnson, R., Brodie, J. P., Forbes, D. A., Ponman, T., 2009, *AJ*, 137, 4956
- Searle, L. Zinn, R. 1978, *ApJ*, 225, 357
- Seigar, M., S., Barth, A. J., Bullock, J. S., 2008, *MNRAS*, 389, 1911
- Sugimoto, D., Chikada, Y., Makino, J., Ito, T., Ebisuzaki, T., Umemura, M., 1990, *Nat*, 345, 33
- Thilker, D. A., Braun, R., Walterbos, R. A. M., Corbelli, E., Lockman, F. J., Murphy, E., Madaena, R., 2004, *ApJL*, 601, 39
- van den Bergh, S., 2000, *The Galaxies of the Local Group*, Cambridge: Cambridge Univ. Press.
- Westmeier, T., Braun, R., Brüns, C., Kerp, J., Thilker, D. A., 2004, *NewAR*, 51, 108